Inorganic Chemistry

ARTICLE

pubs.acs.org/IC

Eu^{3+}-Mediated Polymerization of Benzenetetracarboxylic Acid Studied by Spectroscopy, Temperature-Dependent Calorimetry, and Density Functional Theory

Astrid Barkleit,*[,†,‡] Satoru Tsushima,[†] Olesya Savchuk,[†] Jenny Philipp,[†] Karsten Heim,[†] Margret Acker,[§] Steffen Taut,[§] and Karim Fahmy[†]

[†]Institute of Radiochemistry, Helmholtz-Zentrum Dresden-Rossendorf e.V., P.O. Box 510119, 01314 Dresden, Germany

[‡]Division of Radiochemistry, Department of Chemistry and Food Chemistry, Technische Universität Dresden, 01062 Dresden, Germany

[§]Central Radionuclide Laboratory, Technische Universität Dresden, 01062 Dresden, Germany

Supporting Information

ABSTRACT: Thermodynamic parameters for the complexation of Eu^{3+} with pyromellitic acid (1,2,4,5-benzenetetracarboxylic acid, BTC) as a model system for polymerizable metal-complexing humic acids were determined using temperature-dependent time-resolved laser-induced fluorescence spectroscopy (TRLFS) and isothermal titration calorimetry (ITC). At low metal and ligand concentrations (<50 μM Eu^{3+}, <1 mM BTC), a 1:1 monomeric Eu−BTC complex was identified in the range of 25−60 °C. At elevated concentrations (>500 μM Eu^{3+} and BTC) a temperature-dependent polymerization was observed, where BTC monomers are linked via coordinating shared Eu^{3+} ions. The two methods lead to comparable thermodynamic data ($\Delta H = 18.5 \pm 1.5/16.5 \pm 0.1$ kJ mol^{-1}; $\Delta S = 152 \pm 5/130 \pm 5$ J mol^{-1} K^{-1}; TRLFS/ITC) in the absence of polymerization. With the onset of polymerization, TRLFS reveals the water coordination number of the lanthanide, whereas calorimetry is superior in determining the thermodynamic data in this regime. Evaluating the heat uptake kinetics, the monomer and polymer formation steps could be separated by "time-resolved" ITC, revealing almost identical binding enthalpies for the sequential reactions. Structural features of the complexes were studied by Fourier-transform infrared (FTIR) spectroscopy in combination with density functional theory (DFT) calculations showing predominantly chelating coordination with two carboxylate groups in the monomeric complex and monodentate binding of a single carboxylate group in the polymeric complex of the polycarboxylate with Eu^{3+}. The data show that pyromellitic acid is a suitable model for the study of metal-mediated polymerization as a crucial factor in determining the effect of humic acids on the mobility of heavy metals in the environment.

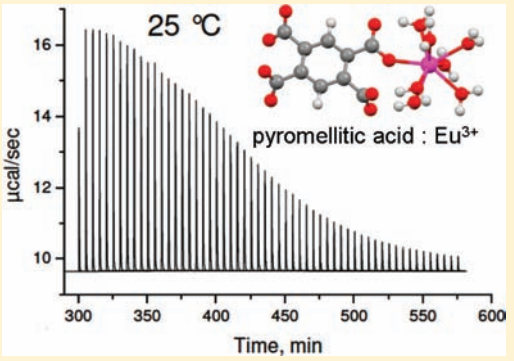

INTRODUCTION

The knowledge of stability constants and thermodynamic data of metal−organic complexes is crucial for both the assessment and the potential attenuation of metal toxicity in the environment. It has gained importance in (radio)ecology of contaminated soils and aquatic systems for thermodynamic modeling of heavy metal and radionuclide migration as well as for novel remediation techniques.[1−8] Here, we derived thermodynamic parameters for the complexation of Eu^{3+} with pyromellitic acid (1,2,4,5-benzenetetracarboxylic acid, BTC) using both time-resolved laser-induced fluorescence spectroscopy (TRLFS) and isothermal titration calorimetry (ITC) at multiple temperatures. BTC mimics the structural arrangement of carboxylates in polyphenols and serves as a model compound for the binding of heavy metals to humic acids.[9,10] The latter are ubiquitous in natural waters and soils, where they affect migration of heavy metal ions through complexation.[1−3,11] The formation of aggregates is typical of humic acids[10] and prevails in pyromellitic acid and related compounds[12−14] emphasizing their suitability as model compounds also with respect to this environmentally important but little investigated property. Usually, TRLFS measurements of Eu^{3+} with humic substances provide only little information; typically a strong quench effect due to the high amount of chromophoric groups in the organic matter is observed.[15,16] Jain et al. could observe only the formation of outer-sphere complexes and found some hints of an inner-sphere complex.[9] These experimental results demonstrate the restrictions of TRLFS in addressing the nature of Eu humate interactions and underline the importance of the investigation of model complexes from which detailed information can be obtained on a molecular level under more favorable experimental conditions.

Received: November 16, 2010
Published: May 23, 2011

Eu^{3+} serves as a model for trivalent lanthanides and actinides. Binding constants are conveniently derived from spectroscopic data following the evolution of characteristic electronic transitions as a function of complex formation. However, deduction of ΔH and ΔS of binding requires determination of the temperature dependence of the binding constant. This limits the applicability of spectroscopy when additional states become populated at elevated temperatures, and spectroscopy may not be applicable at all when scattering accompanies the thermally activated build up of polymeric complexes. Metal-mediated aggregate formation, however, is of salient importance for environmental toxicity, because it strongly affects bioavailability. Previous spectroscopic studies on Eu−BTC complexes have been restricted to conditions which prevent polymerization, i.e., low complex concentrations and ambient temperatures,[17] but studies of complex formation at variable temperatures are essential because the chemical speciation and metal mobility in soils strongly depend on varying environmental conditions.[4,18,19]

Here, we extend previous TRLFS and calorimetric studies on the Eu−BTC complex[17,20] to elevated temperatures and concentrations. We identify the limits within which thermodynamic parameters derived from temperature-dependent TRLFS are consistent with the direct measurement of reaction heats by ITC. Beyond these limits, TRLFS fails to describe binding equilibria but retains its predictive power with respect to coordination chemistry. However, the separation of the thermodynamic parameters of Eu−BTC complex formation and the subsequent polymerization under environmentally more realistic conditions can only be achieved by ITC. In addition to the determination of the number of water coordination sites around Eu^{3+} by TRLFS, the type of carboxyl interactions was investigated by Fourier-transform infrared (FTIR) spectroscopy in combination with density functional theory (DFT) calculations. The IR data reveal a heterogeneous origin of the prevalent monodentate coordination of Eu^{3+} in the polymerized complexes. The data provide a comprehensive picture of the structure and thermodynamics of the Eu−BTC complex which represents a realistic model system for environmentally relevant Ln^{3+} and An^{3+} complexes with humic substances.

EXPERIMENTAL SECTION

Solutions and Reagents. Eu_2O_3, $EuCl_3 \cdot 6H_2O$, and pyromellitic acid were purchased from Aldrich and used without further purification. The ionic strength was kept constant for all experiments at 0.1 M by adding stock solutions from $NaClO_4 \cdot H_2O$ or NaCl (Merck, p.A.). Necessary pH adjustments were carried out with 1, 0.1, or 0.01 M NaOH or $HClO_4$ with an accuracy of 0.02 units; pH values were measured with a BlueLine 16 pH electrode (Schott).

Potentiometric Titration. Samples were prepared in an inert gas box (nitrogen) with carbonate-free deionized water. The measurements were carried out at CO_2-free conditions under a nitrogen atmosphere in 0.1 M $NaClO_4$ as an acid−base titration. Thirty milliliter samples of 0.01 M BTC (initial pH 2.0) were automatically titrated (736 GP Titrino/TiNet 2.50, Metrohm) with 0.1 M NaOH (carbonate free, Titrisol, Merck) at temperatures between 25 and 60 °C (see Table 1). Dynamic titration was used with a minimum drift of 0.5 mV/min and a delay time of at least 60 s at each point before measuring the pH with a Schott BlueLine 11 pH combination electrode with a platinum diaphragm. The electrode was calibrated for each experimental run with NBS standard buffers (pH 4.008 and 6.865, Schott). Titrations were done in triplicate between pH 2 and 7 at each temperature and analyzed using the program HYPERQUAD2006.[21]

Table 1. pK_a Values and Thermodynamic Data of BTC (in 0.1 M $NaClO_4$) at Varying Temperatures Determined by Potentiometric Titration

	pK_{a1}	pK_{a2}	pK_{a3}	pK_{a4}
25 °C	1.92 ± 0.03	2.77 ± 0.03	4.36 ± 0.02	5.35 ± 0.02
	1.70[20]	2.63[20]	4.18[20]	5.25[20]
		3.12[34]	4.92[34]	6.23[34]
30 °C	1.91 ± 0.02	2.86 ± 0.01	4.45 ± 0.01	5.43 ± 0.01
40 °C	2.05 ± 0.02	2.88 ± 0.01	4.48 ± 0.01	5.48 ± 0.01
50 °C	2.11 ± 0.01	2.88 ± 0.01	4.47 ± 0.01	5.51 ± 0.01
60 °C	2.13 ± 0.02	2.91 ± 0.02	4.50 ± 0.01	5.50 ± 0.02
ΔH (kJ mol^{-1})	13.2 ± 2.2	6.0 ± 2.2	6.0 ± 2.4	7.7 ± 2.3
	13.0[a20]	6.8[a20]	1.3[a20]	4.5[a20]
		6.6[a34]	3.3[a34]	6.7[a34]
ΔS (J mol^{-1} K^{1})	81 ± 7	74 ± 7	104 ± 8	129 ± 8
	76[a20]	73[a20]	84[a20]	116[a20]
		82[a34]	106[a34]	142[a34]

[a] From calorimetry (25 °C).

Table 2. Complex Stability Constants at Varying Temperature for the Monomeric 1:1 Eu−BTC Complex (in 0.1 M $NaClO_4$) Determined by TRLFS

T/°C	log β
25	4.70 ± 0.06
	4.86 ± 0.03[a20]
30	4.75 ± 0.12
40	4.89 ± 0.07
50	4.97 ± 0.11
60	5.03 ± 0.06

[a] From potentiometric titration.

Isothermal Calorimetric Titration (ITC). ITC measurements were done with a Microcal VP-ITC calorimeter (GE Healthcare, Buckinghamshire, U.K.) at different temperatures (25, 40, and 60 °C). A total of 56 aliquots (5 μL of 10 mM BTC in 0.1 M $NaClO_4$, pH 5.7) was injected in 1.412 mL of 1 mM $EuCl_3$ (0.1 M $NaClO_4$, pH 5.7) in 5 min intervals at 25 °C and in 27 min intervals at 40 and 60 °C to allow completion of slow reactions at these temperatures. Where appropriate, the measurements were corrected for the heat of dilution of the titrant, determined in separate runs. Measurements were analyzed with the associated software Origin 7.5.[22]

Time-Resolved Laser-Induced Fluorescence Spectroscopy (TRLFS). Luminescence spectra were recorded using a pulsed flash lamp pumped Nd:YAG-OPO laser system from Continuum (Santa Clara, CA) as described.[23] Excitation was at 395 nm, and a constant time window of 1 ms was used for all measurements. Static and time-dependent luminescence spectra of Eu^{3+} were recorded at 565−650 (1200 line mm^{-1} grating, 0.2 nm resolution, 2000 accumulations) and 440−780 nm (300 line mm^{-1} grating, 0.7 nm resolution, 200 accumulations), respectively. For time-resolved measurements, 41 spectra were recorded with 15 μs separation. Spectrophotometric titrations were done at least in triplicate starting with 30 μM Eu^{3+} in 0.1 M $NaClO_4$ at pH 5.0. Subsequent additions of aliquots of a 0.01 M BTC stock solution (0.1 M $NaClO_4$, pH 5.0) covered BTC concentrations from 10 μM to 1 mM. At least 20 spectra each were measured in the 25−60 °C range (see Table 2) using a stirred temperature-controlled cuvette holder (Flash 300, Quantum Northwest, U.S.A.) and 30 min initial equilibration time and an additional 10 min after each injection of BTC at a given

dx.doi.org/10.1021/ic102292j |Inorg. Chem. 2011, 50, 5451–5459

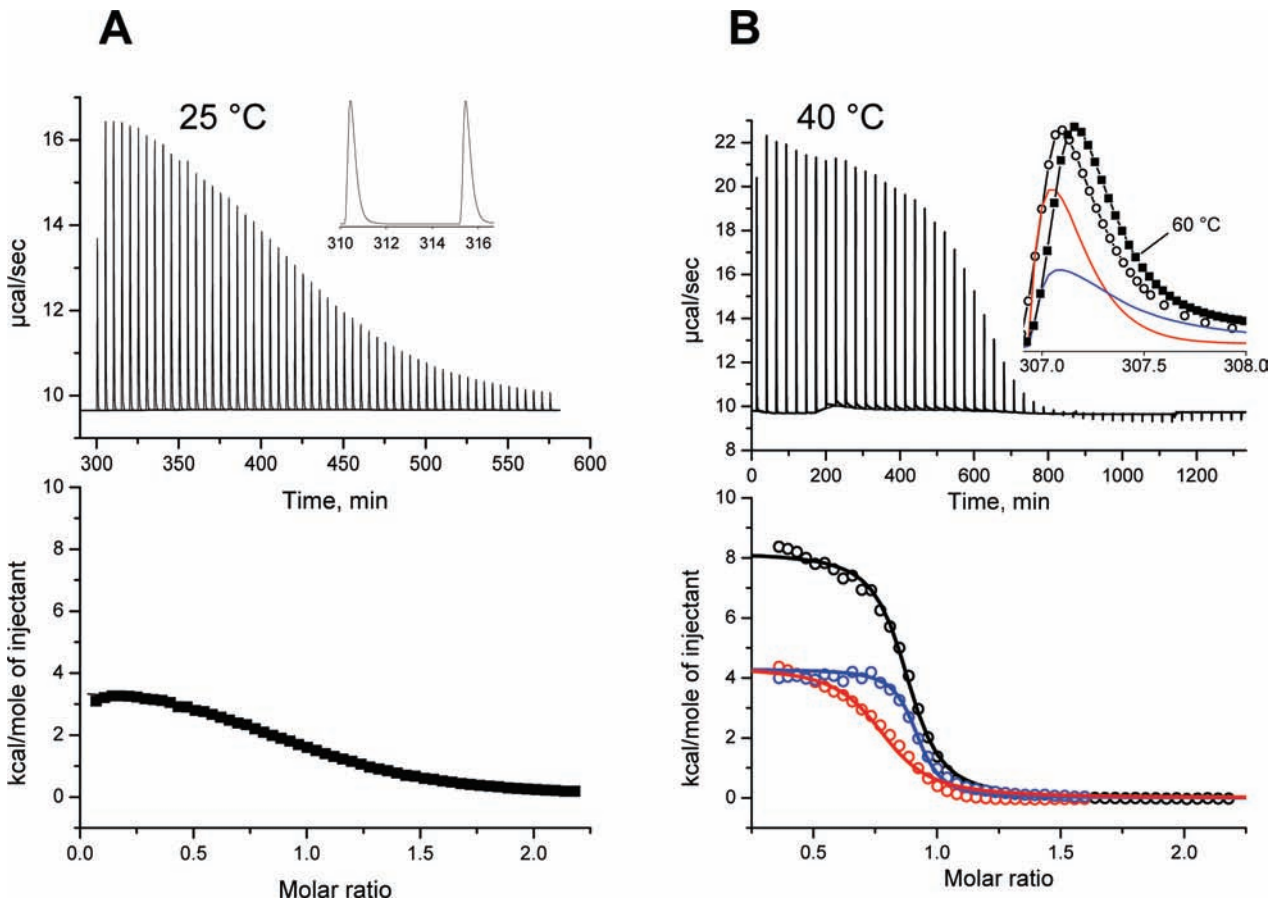

Figure 1. Heat uptake during Eu−BTC complex formation measured by isothermal titration calorimetry. (A) Complex formation upon injection of BTC at 25 °C is characterized by fast transients of heat uptake (top) that are complete within less than 2 min (inset). The integrated heats (bottom) are consistent with a 1:1 stoichiometry and ΔH and ΔS values of 16.5 ± 0.1 kJ mol^{-1} and 130 ± 5 J mol^{-1} K^{-1}, respectively. (B) (Top) Complex formation upon injection of BTC at 40 °C is characterized by a prolonged heat uptake (inset, open circles) which can be decomposed into a fast (inset, red) and slow (inset, blue) component. The prolonged uptake becomes further pronounced with increasing temperature (filled squares, corresponding to 60 °C). (Bottom) Corresponding to the fast and slow responses, the total integrated heats (black) can be reproduced from the sum of the fast (red) and slow contributions (blue). The resulting curves are both consistent with a 1:1 stoichiometry. ΔH for the fast and slow reaction is 14.6 ± 0.4 and 16.3 ± 0.4 kJ mol^{-1} K^{-1} with ΔS of 138 ± 4 and 160 ± 4 J mol^{-1} K^{-1}, respectively. All experiments were carried out with an initial concentration of 1 mM Eu^{3+}.

temperature. Spectra were normalized to the peak area of the $^5D_0-^7F_1$ transition. Stability constants of the Eu−BTC complexes were determined based on the decomposition of the static luminescence spectra into spectral components assigned to free and complexed Eu^{3+} via factor analysis using Specfit.[24] For a predefined stoichiometry, the program calculates the complex stability constants using the Levenberg−Marquardt algorithm, a numerical solution to the problem of minimizing a nonlinear function with least-squares curve fitting. Consistency of the stoichiometry is addressed experimentally by analyzing the linear relation between the chemical potential difference of the free and complexed Eu^{3+} versus that of free BTC (see Figure 3 and Results/TRLFS section).

Time-resolved spectra were analyzed with Origin 7.S[22] using the 570−630 nm range (similar to the spectral range of static spectra) to obtain the luminescence lifetimes τ. The number N of water molecules in the Eu^{3+} coordination shell was calculated according to Kimura et al.[25] as

$$N(\pm 0.5) = 1.07/\tau(\text{ms}) - 0.62 \quad (1)$$

Fourier-Transform infrared (FTIR) Spectroscopy. FTIR spectra were recorded in aqueous phase using a Vector-22 spectrometer (BRUKER, Karlsruhe, Germany) equipped with a diamond attenuated total reflectance (ATR) unit (RESULTEC, Illerkirchberg, Germany). The ligand was measured at pH 7.0 and 100 mM BTC. For the polymer solution, 20 μL of 100 mM $EuCl_3$ solution (pH 7.0) was mixed with 20 μL of a 100 mM BTC solution (pH 7.0), resulting in a final concentration of 50 mM Eu^{3+} and BTC each. The mixture precipitates rapidly and was therefore measured as a suspension. The Eu−BTC monomeric complex was measured at pH 5.0, 1 mM Eu^{3+}, 1 mM BTC, and 0.1 M NaCl in a flow cell (volume 200 μL) with a constant flow rate of 200 μL/min and the absorption difference calculated from the spectra of the complex and the pure ligand. For every single spectra 4 × 256 scans were coadded. Spectral resolution was 2 cm^{-1}. Water single-channel spectra were used as a reference to calculate absorption spectra.

Density Functional Theory (DFT) Calculation. DFT calculations were performed using Gaussian 03.[26] Geometries were optimized in the aqueous phase at the B3LYP level using the CPCM solvation model[27] with UAHF radii.[28] The large core effective core potential (LC-ECP) as well as the corresponding basis set suggested by Dolg et al. was used on Eu.[29] For C, O, and H, all-electron valence triple-ζ basis set plus polarization and diffuse functions have been used.[30] The LC-ECP used in this study is specifically designed for the trivalent Eu incorporating six unpaired 4f electrons into the core potential, thereby enabling "closed-shell" calculations on Eu^{3+}, which has the formal electronic

dx.doi.org/10.1021/ic102292j |Inorg. Chem. 2011, 50, 5451–5459

Table 3. Summary of the Thermodynamic Data for the 1:1 Eu−BTC Complex

T/°C	$\Delta_r H$/kJ mol^{-1}	$\Delta_r S$/J mol^{-1} K^{-1}	$\Delta_r G$/kJ mol^{-1}	method
25−60	18.5 ± 1.5	152 ± 5	−26.8 (25 °C)[a]	TRLFS
25	17.0 ± 1.6[20]	150 ± 1[20]	−27.7[20]	ITC[20]
25	16.5 ± 0.1[b]	130 ± 3	−22.2	ITC
40	34.2 ± 0.3[b]	210 ± 9	−31.5	ITC
60	46.9 ± 0.2[b]	247 ± 9	−35.4	ITC

[a] Calculated with the formula $\Delta_r G = \Delta_r H - T\Delta_r S$. [b] $\Delta C_p = 0.9$ kJ mol^{-1} K^{-1} was calculated from $\Delta H/\Delta T$.

configuration of the septet spin state. This simplification is justified because the 4f orbital is strongly contracted, shielded by valence orbitals, and does not participate in the chemical bond between Eu^{3+} and the ligand. The final geometries were confirmed to be the energy minimum through vibrational frequency analysis where no imaginary frequency was found to be present. The vibrational spectra were fitted with the half-width of 8 cm^{-1} at half-height using the calculated harmonic frequencies and IR intensities.

The spin−orbit effect and multiconfigurational character of the system were neglected. Both effects are expected to be important for the accurate determination of the electronic energy levels of the Eu^{3+} complex. Their contributions to the ground state geometry, however, are small because 4f electrons are localized on the Eu atom in the ground state and low-energy excited states and do not contribute to ligand interactions. According to the recent study on Cm^{3+} complexes,[31] which are analogous to the Eu^{3+} complexes, solvation energy is the most critical factor for determination of geometries and vibrational frequencies. The first coordination sphere around Eu was saturated with water molecules fixing the coordination number to 8 or 9. The rest of the solvation shells were also considered through the use of the CPCM model. Since our focus is exclusively on geometry and vibrational frequencies, the approach is sufficiently accurate and has been used by others.[32,33]

RESULTS

Potentiometric Titration. In addition to the proton dissociation constants of BTC at 25 °C[20,34] those at higher temperatures are required here for determination of complex stability under polymerizing conditions, i.e., at elevated temperatures. Table 1 summarizes the dissociation constants for the pyromellitic acid at 25−60 °C. For 25 °C, our data are within the diverging range of reported values.

From the temperature-dependent pK_a values the enthalpy and entropy of protonation can be derived from the van't Hoff equation in a modified linear form

$$\ln K = -\frac{\Delta H}{R}\cdot\frac{1}{T} + \frac{\Delta S}{R} \qquad (2)$$

The obtained data are listed in Table 1 and correlate well with published calorimetric data at 25 °C.[20,34]

Isothermal Titration Calorimetry. Isothermal calorimetric titration experiments were carried out at 25, 40, and 60 °C (Figure 1). All ITC traces showed endothermic binding of BTC to Eu^{3+} and the corresponding binding stoichiometries obtained from single site fits where 1.0, 1.2, and 0.9, respectively. At 25 °C, the reaction enthalpy ΔH is 16.5 kJ mol^{-1} and the entropy ΔS is 130 J mol^{-1} K^{-1} as derived from the ITC data in Figure 1A. These numbers are in very good agreement with literature data[20] (Table 3). The endothermic ITC response at 25 °C was complete within less than 2 min (Figure 1A, inset). With rising temperature, however, it became biphasic with a "tailing heat uptake" resulting in an apparent ΔH of 34.2 kJ mol^{-1} (ΔS = 210 J mol^{-1} K^{-1}), i.e., close to twice the molar enthalpy observed at 25 °C (Figure 1B). This indicates that at higher temperatures an additional reaction succeeds the fast binding event. Figure 1B exemplifies the biphasic behavior at 40 °C by decomposing the ITC signal into a fast component with similar kinetics as measured at 25 °C and a slower phase that covers the extended heat uptake observed at higher temperatures. The slow phase becomes further pronounced at 60 °C (Figure 1B, inset). Instead of the classical evaluation of the ITC curve using a single binding reaction, it is thus reasonable to assess the reaction heat separately in different time windows. It is indeed possible to split the total heat uptake into the sum of the two isotherms shown in Figure 1B (lower panel). With increasing amounts of Eu^{3+}, the heat taken up in the early phase (i.e., within the first 30 s) is successively reduced in relation to that absorbed over the following time. This indicates that the binding reaction underlying the fast component saturates earlier than the ensuing reaction. Remarkably, the integrated heats of the early and late phase of the transient can be modeled with individual enthalpies of 14.6 and 16.3 kJ mol^{-1} (with reaction entropies of 138 and 160 J mol^{-1} K^{-1}, respectively, and a stoichiometry of 0.8−0.9). These values are very close to those of the 1:1 binding reaction at 25 °C. Therefore, the data indicate that at temperatures above 40 °C, the slow heat release that follows formation of the Eu−BTC 1:1 complex originates in an ensuing second Eu^{3+}-coordinating interaction with thermodynamic parameters very similar to those of the fast initial complex formation. In accordance with the onset of visually observable precipitation at 40 °C, the additional Eu^{3+} coordination appears to be crucial for the formation of polymeric states. Remarkably, the ITC data demonstrate that at 40 °C an overall 1:1 stoichiometry also holds for the polymerized Eu−BTC complexes. This hints at a polymerization process in which the previously bound Eu^{3+} ions in the monomeric complexes are shared between BTC molecules, rather than multimer formation by additional incorporation of metal ions. Although consistent with the revealed stoichiometry, the structural implications of this second reaction step cannot be inferred from calorimetry but become evident by comparison of time-resolved laser-induced fluorescence spectra recorded under conditions that either prevent or favor formation of polymerizing states.

Time-Resolved Laser-Induced Fluorescence Spectroscopy. To address structural differences in Eu coordination in a 1:1 stoichiometry realized either with a BTC monomer or within a polymeric state, we applied time-resolved laser fluorescence of the different Eu−BTC complexes. Figure 2A shows the spectrophotometric titration of Eu^{3+} with BTC at 25 °C. With increasing ligand concentration, a strong increase of the intensity of the emission by the hypersensitive $^5D_0-{}^7F_2$ transition at 615 nm is observed. The appearance of the formally forbidden $^5D_0-{}^7F_0$ transition at 579 nm indicates deformation of the first hydration shell of the Eu^{3+} ion upon complexation. Irrespective of the BTC concentration, the luminescence exhibits a monoexponential decay despite the intrinsically different decay times for the fully hydrated and coordinated Eu^{3+} ion. Due to a fast kinetic equilibration at room temperature, the observed apparent lifetime is actually a mixture of the decay rates of the excited states of both the uncomplexed and the complexed Eu species.[35] At 25 °C, the initial luminescence lifetime of 111 ± 4 μs, which is typical of the Eu^{3+}(aq) ion,[25,36−38] increases to a constant value of 135 ±

dx.doi.org/10.1021/ic102292j |Inorg. Chem. 2011, 50, 5451–5459

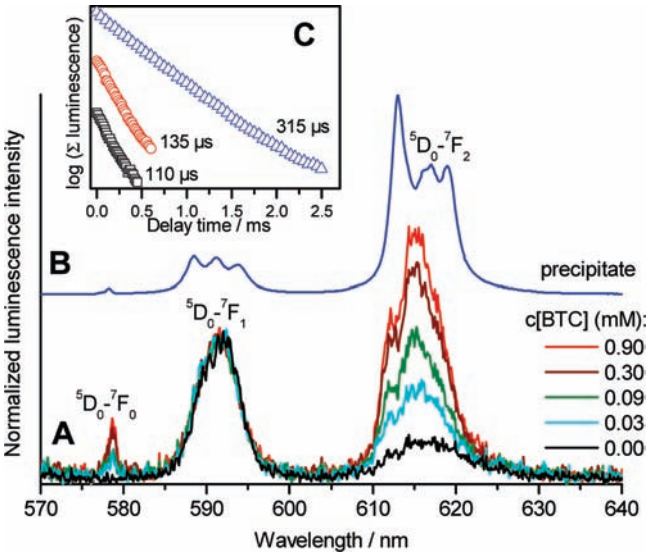

Figure 2. Luminescence properties of Eu−BTC complexes. (A) Selected emission spectra of the spectrophotometric titration of 30 μM Eu^{3+} with BTC (25 °C, pH 5.0). (B) Luminescence of the precipitate forming at 1 mM Eu^{3+} and 1 mM BTC (40 °C, pH 5.7). (C) Luminescence decay traces and corresponding lifetimes of Eu^{3+}(aq) (black), Eu−BTC aqueous complex at 30 μm Eu^{3+}, 4.5 mM BTC, 25 °C, pH 5.0 (red), and the Eu−BTC precipitate (composition like B) (blue).

3 μs (averaged) with more than 60-fold excess of BTC. A similar lifetime for the Eu−BTC system was measured by Wang et al.[17] In contrast to the ITC traces, the measured luminescence lifetimes did not depend on temperature between 25 and 60 °C (see Table S1, Supporting Information) and the samples did not exhibit precipitation, indicating that polymeric states are not formed at the lower Eu^{3+} concentrations used in these TRLFS experiments. The number of water molecules coordinating the unbound Eu^{3+} ion is 9.0 ± 0.5 as derived from the related luminescence lifetime at 25 °C and 9.2 ± 0.5 at 60 °C (τ = 109 ± 1 μs), whereas the prolonged luminescence lifetime of the Eu−BTC complex agrees with the presence of 7.3 ± 0.5 (25 °C) to 7.5 ± 0.5 (60 °C, τ(av) = 130 ± 2 μs) water molecules. Thus, 1−2 water molecules are replaced by the carboxyl oxygens upon coordination by BTC. In a 1:1 Eu−BTC complex, this would agree with the formation of either a monodentate, a chelate or a bidentate complex of Eu with two carboxyls (attached to the same BTC molecule) or with a single carboxyl group, respectively. Comparable TRLFS data have been obtained for the recently studied Am^{3+}−BTC 1:1 complex.[39]

The TRLFS measurements were carried out at more than 30-fold lower Eu^{3+} concentration than the ITC experiments. Thereby, the conditions allow deriving the binding enthalpy and entropy from the temperature dependence of the spectroscopically determined binding constant unperturbed from scatter artifacts which arise from polymerization at higher temperatures.

From the general formula of complex formation

$$Eu^{3+} + nBTC^{x-} \rightleftarrows Eu(BTC)_n^{(3-nx)+} \quad (3)$$

it follows that

$$\log([Eu(BTC)_n^{(3-nx)+}])/([Eu^{3+}]) = n\cdot\log[BTC^{x-}] + \log K \quad (4)$$

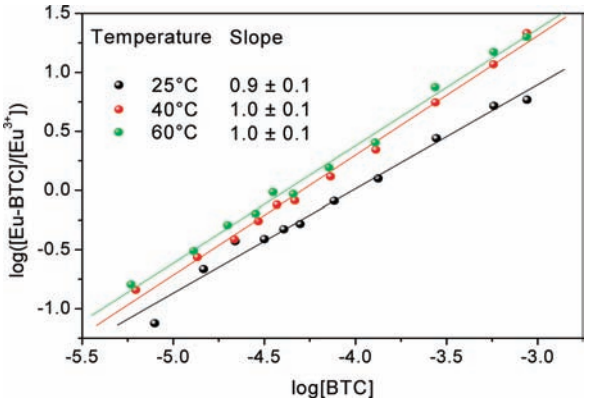

Figure 3. Spectrophotometrically determined dependence of the Eu−BTC:Eu^{3+} concentration ratio on the concentration of uncomplexed BTC at various temperatures at pH 5.0 according to eq 4, resulting in the stoichiometric factor n (slope). Only one measurement series per temperature was depicted.

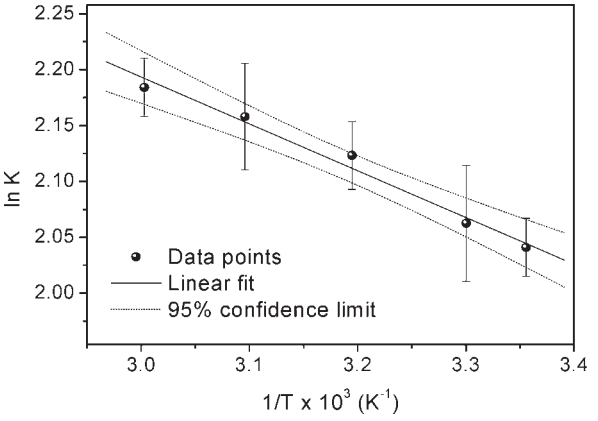

Figure 4. van't Hoff plot of the Eu−BTC complex formation (from TRLFS at 30 μM Eu^{3+}, 30 μM to 1 mM BTC, pH 5.0, I = 0.1 M $NaClO_4$, 25−60 °C).

with K being the association constant. The left side of eq 4 can be obtained from the band shape analysis of the luminescence spectra of the solvated Eu^{3+} ion and the complexed lanthanide saturation with excess of BTC as basis spectra to deduce n and K from the spectroscopic titration (see Experimental Section). Figure 3 shows the linear relation expressed in eq 4 revealing a stoichiometry of the Eu−BTC complex close to 1:1 at all temperatures. This is in accordance with the literature.[17,20] Formation of 2:1 (or even higher) Eu−BTC complexes is very unlikely; those complexes have been reported only at very high metal ion concentrations (10^{-2}−1 M) and at a high excess of the metal ion over the ligand[40,41] Also, formation of ML_2 or ML_3 complexes is very unlikely. It has not been observed until now for lanthanides even with high ligand excess.[17,20]

The complex stability constants are summarized in Table 2. The stability constant (log β) is 4.70, significantly higher than those for benzenemono- (∼2), -di- (2−3), or -tricarboxylates (3−4).[17] This is in accordance with the higher basicity of the ligand BTC (as reflected by the sum of the protonation constants) and is expected for systems involving hard acid−hard base interactions.[20] The stability constant increases with temperature in agreement with the endothermic reaction enthalpy.

dx.doi.org/10.1021/ic102292j |Inorg. Chem. 2011, 50, 5451–5459

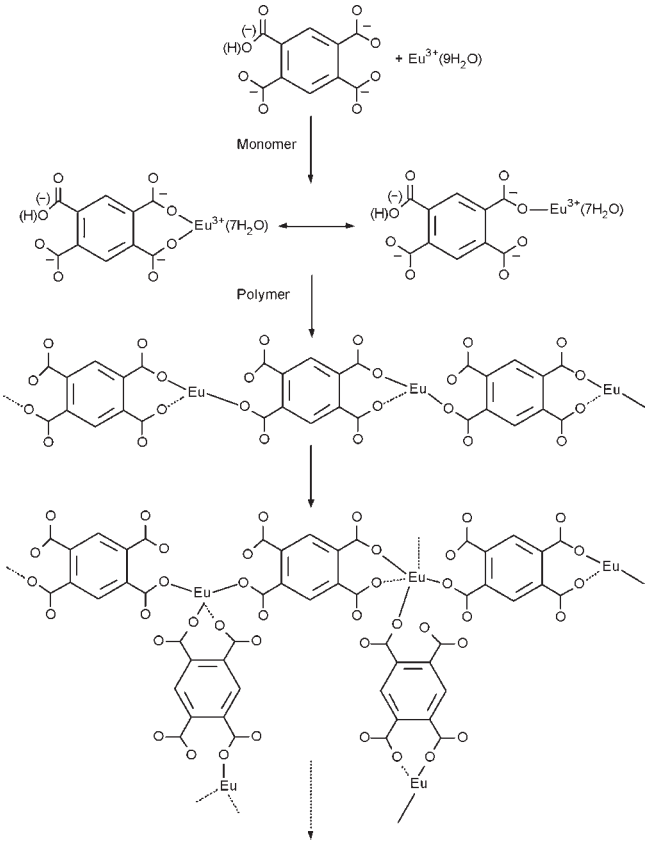

Figure 5. Schematic description of the stepwise formation of the Eu−BTC polymer demonstrating possible chelating and monodentate binding modes and the prevalence of a 1:1 stoichiometry in both the monomeric and the polymeric states. For clarity, charges, protons, and water molecules are omitted in the polymeric structures. The likely formation of three-dimensional networks is not ruled out, and its experimental analysis is beyond the scope of the present manuscript.

The linearity of the van't Hoff plot in Figure 4 further shows that also the enthalpy of complex formation is virtually independent of temperature (18.5 kJ mol^{-1}) and together with the obtained reaction entropy of 152 J mol^{-1} K^{-1} agrees with both published data[20] and the ITC results reported here (Table 3).

To prevent scattering, spectroscopic determination of the binding constants required suppression of polymerization which was achieved at Eu^{3+} concentrations below 50 μM. Above pH 7, carbonate and hydroxide species became dominant as judged from the Eu^{3+} luminescence spectra and lifetimes (data not shown), and at Eu^{3+} concentrations above 500 μM equimolar amounts of BTC added at neutral pH caused aggregation. At 40 °C and millimolar concentrations of both BTC and Eu^{3+}, aggregates formed even at pH 5.7. Thus, the experimental regime used for ITC cannot be applied for the TRLFS-based determination of binding constants. On the other hand, aggregated states of metal-loaded humic acids are environmentally important as they determine metal mobility. Therefore, the study of the Eu−BTC model complex under aggregate-forming conditions allows addressing a salient property of the structurally more complex humic acids. Although association constants for aggregate formation cannot be deduced from TRLFS, spectral analysis of the polymeric form is possible. Figure 2 compares the luminescence spectra of aggregates formed at equimolar concentration (1 mM) of Eu^{3+} and BTC at pH 5.7, 40 °C with those of the soluble complex. The $^5D_0-^7F_0$ peak (578 nm) is less pronounced in the aggregate, indicative of a more symmetrical structure than in solution. We ascribe this to formation of multimeric states in which the majority of Eu^{3+} ions is shared by two BTC molecules. Under these conditions, any 2 adjacent BTC molecules are bridged by a shared Eu^{3+} ion. Thereby, a more symmetrical ("bilateral") coordination with 2 carboxyl oxygens from each BTC molecule can be provided in a planar arrangement as compared to the less symmetric ("unilateral") coordination by carboxyl oxygens in the monomeric complex. The lifetime of Eu^{3+} luminescence in the multimeric state increases to 205 ± 3 (pH 7.0, 25 °C) and 315 ± 5 μs (pH 5.7, 40−60 °C), respectively, corresponding to 4.5 ± 0.5 and 2.8 ± 0.5 coordinating water molecules which implies the additional exchange of 2−4 water molecules upon polymerization of the monomeric complex. The reduced coordination number for water under polymerizing conditions fully confirms the structural interpretation of Eu^{3+}-bridged BTC polymers with sharing of the lanthanide between neighboring BTC molecules. Thereby, the calorimetrically derived overall 1:1 stoichiometry also in the polymeric state can be fully rationalized. Figure 5 symbolizes the proposed polymeric structure and stoichiometry.

Vibrational Spectroscopy and DFT Analysis. In an attempt to relate the most prominent experimentally determined vibrational features to those derived from DFT calculations for specific coordination modes, the structures of monomeric and polymeric Eu−BTC complexes were assessed by FTIR spectroscopy at room temperature and compared with DFT calculations. It should be noted that the DFT calculations were used here to assign IR bands to the most likely predominant coordination modes, and only the 1:1 Eu−BTC complex has been calculated by DFT. The structures and IR spectra of Eu−BTC complexes were calculated with different coordination numbers (CN) of 8 and 9 and also with different coordination modes (monodentate, bidentate, and chelate ring formation). The structures and relative Gibbs energy including the solvation energy are shown in Figure S1 in the Supporting Information. In both monodentate and bidentate complexes, the CN 8 was found to be more stable than the CN 9 by 44.6 and 33.1 kJ/mol, respectively, which is a clear indication of CN 8 prevalence over CN 9. For the chelate ring complex, the energy difference between CN 8 and CN 9 is only 11.6 kJ/mol and thus too small to identify a unique CN. It can also be seen in Figure S1, Supporting Information, that the energy differences among the complexes with different coordination modes and CN 8 are overall small. They all lie within the energy difference of 5 kJ/mol and do not allow identifying a predominant coordination mode on purely theoretical grounds. It will be shown, however, that the FTIR results in combination with TRLFS data allow proposing the structural model that is most consistent with both DFT and spectroscopy.

Figure 6 shows the experimental and theoretical IR spectra of free BTC (Figure 6A) and BTC complexed with Eu^{3+} (Figure 6B, monomer; Figure 6C, polymer). In DFT calculations, we calculated IR spectra of the complexes with three different coordination modes (monodentate, bidentate, and chelate) and two different CN (8 and 9) which are given in Figure S2 in the Supporting Information. Structural conclusions are based on the carboxylate vibrations as they are the most sensitive to the coordination mode. The comparison of the data of the free ligand (Figure 6A) shows that the relative positions and intensities of the calculated vibrational bands are in good

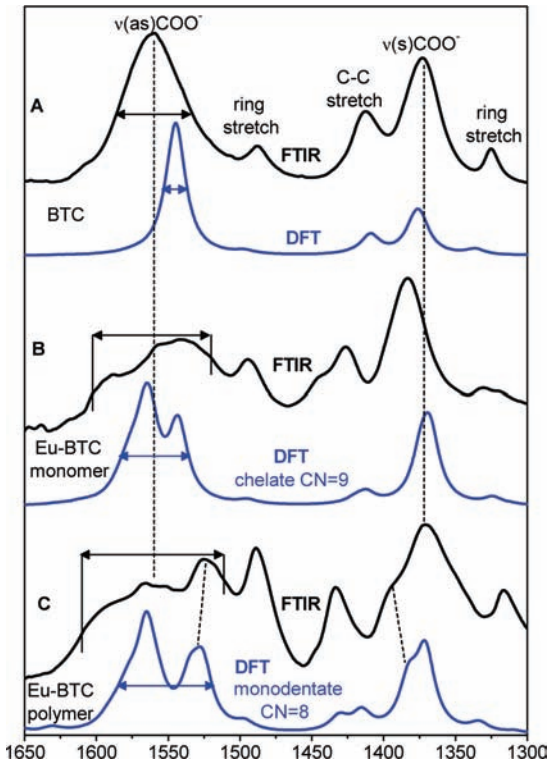

Figure 6. Comparison of experimental (black) and theoretical IR spectra (blue, derived from DFT calculations of BTC and Eu−BTC complexes). (A) BTC in 0.1 M $NaClO_4$ without europium. (B) Eu−BTC complex under conditions of a prevalent monomeric state of 1:1 stoichiometry. (C) Eu−BTC complex under polymerizing conditions with 1:1 stoichiometry. The assignment to the dominating molecular structure is based on the successive broadening of the ν(as)COO^- vibrational modes (arrows indicate bandwidths at half-maximum). This splitting/broadening is best reproduced by the DFT calculations for the indicated structures and takes into account consistency with the TRLFS data. Vertical dotted lines mark the ν(as)COO^- and ν(s)COO^- stretching frequencies on which the structural interpretations are based.

accordance with the measured spectrum. DFT calculation shows that Eu^{3+} binding splits either the asymmetric (1550−1600 cm^{-1}; monodentate or chelate) or the symmetric (1350−1400 cm^{-1}; bidentate) carboxylate band of BTC, leading to broad overlapping bands between 1520 and 1600 cm^{-1} and from 1350 to 1400 cm^{-1}, respectively (see Figure S2, Supporting Information). The bidentate coordination does not cause band splitting of the asymmetric COO^- stretch but strongly shifts it to lower frequency, whereas splitting is observed for the symmetric stretch. Due to the broad absorption bands in the experimental spectra, such shifts and splittings will affect mainly the total bandwidth in the 1500−1600 cm^{-1} range. The ν(as)COO^- stretches clearly cover a larger frequency range in the Eu−BTC monomer (Figure 6B) than in the free ligand (Figure 6A). The increased absorption above and below the ν(as)COO^- of the additionally present free carboxylate (Figure 6, dotted line) indicates that splitting does indeed occur upon monomer formation. Thus, a bidentate coordination can be ruled out. Also, the two energetically most preferred binding modes, the chelate and bidentate complexes with CN 8, each can be ruled out at least for the monomeric form due to the TRLFS results. These coordination modes would retain 6 water molecules in the first coordination shell of Eu^{3+}. This is contrary to TRLFS findings, where we found that 7−8 water molecules remain after complexation. Instead, the two DFT spectra which agree best with experiment are shown in Figure 6. These are the chelate complex with CN 9 corresponding best with the monomer absorption (Figure 6B) and the monodentate complex with CN 8 corresponding best with the polymer (Figure 6C). In the latter, the splitting is even broader (as is the total bandwidth in the experimental spectra) leading to a more distinct low-frequency ν(as)COO^- stretch at 1530 cm^{-1} also seen experimentally. Additionally, a high-frequency shoulder is produced in the ν(s)COO^- band in both the calculated and the measured spectra. These most likely predominant coordination modes take also into account our TRLFS data which show that a chelating coordination requires a CN 9 and 7−8 water molecules still reside in the first coordination shell of Eu^{3+} in the monomeric complex. The large experimental bandwidth indicates that multiple coordination modes exist in both the monomer and the polymer (see Figure 5). Indeed, the binding mode of the Eu−BTC polymer is thus consistent with the structure of the terbium (Tb^{3+}) polymer with 1,4-benzenedicarboxylic acid (BDC) which shows monodentate cross-linking of 1:1 Tb−BDC units.[42]

DISCUSSION

We determined the thermodynamic parameters of the Eu−BTC complex by temperature-dependent TRLFS and compared the results with those from isothermal calorimetric experiments. At 25 °C both methods show an entropy-driven endothermic 1:1 complex formation (Table 3), and the obtained parameters are in excellent agreement with published data.[20] Whereas entropy and enthalpy of the complex formation are independent of temperature at micromolar complex concentrations as revealed by TRLFS, the ITC data recorded at ∼1 mM concentrations show an increase with temperature and a biphasic heat uptake above 40 °C, indicative of two consecutive reaction steps. Under these conditions TRLFS cannot address the thermodynamics due to increased scatter from Eu−BTC aggregates. Nevertheless, it evidences the additional displacement of 2−4 water molecules in the Eu^{3+} hydration shell in the aggregated state. On average, at least 4 or even up to 6 carboxylate oxygens coordinate the lanthanide instead of only 1 or 2 in the low-temperature low-concentration regime. However, 1:2 or 1:3 stoichiometries do not comply with the ITC result, because the heat uptake saturates already at a molar ratio of one, despite the fact that indeed about twice the heat is taken up as compared to the 1:1 complex at 25 °C (Figure 1B). The apparently contradicting results can be reconciled by the initial fast formation of a "monomeric" 1:1 complex followed by the slower "head-to-tail-like" addition to another monomer or previously formed polymers providing the additional carboxyl oxygens for coordination of the linking Eu^{3+} ion shared by the adjacent BTC molecules. Figure 5 shows how linear or branched polymers of an overall 1:1 stoichiometry can thus form. Both the initial monomeric Eu−BTC formation and the Eu^{3+}-mediated linkage to another Eu−BTC unit involve the approach of 2 carboxyl oxygens and the corresponding displacement of about 2 water molecules from the coordination shell of the Eu^{3+} ion, reducing the number of coordinating water molecules from ∼9 to ∼7 and from ∼7 to ∼5, respectively. Energetically, both processes are remarkably similar, leading to about twice as large

dx.doi.org/10.1021/ic102292j |Inorg. Chem. 2011, 50, 5451–5459

molar enthalpy and entropy changes with the onset of polymerization. The free energy of the local electrostatic (0.75−1 formal negative charge per free carboxyl at pH 5.7 in both BTC and the Eu−BTC complex) and coordinative binding interactions of Eu^{3+} at the carboxyl oxygens are thus rather independent of the overall charge state of BTC (∼3.5 at pH 5.7) or Eu−BTC (about neutral to anionic at pH 5.7). Long-range electrostatic contributions to Eu^{3+} binding are further screened by the ionic strength of the medium and the polymer formation favored by the neutral state of the Eu−BTC monomers. We ascribe the entropy increase upon Eu^{3+} coordination to the release of water from the inner coordination shell. In line with this interpretation, the entropy gain scales with the release of ∼2 and ∼4 water molecules in the mono- and polymeric states, respectively.

The proposed structural model provides a consistent explanation for the stoichiometry and heat uptake measured by ITC as well as for the spectral properties of the lanthanide coordinated in the monomeric or polymeric state. The data are thus consistent with formation of metal-linked polymers as described for benzenemulticarboxylates[12,42−45] and several polymeric lanthanide BTC complexes,[13,14,46,47] where also mainly a 1:1 metal-to-ligand stoichiometry is observed.

The assignment of the experimental IR frequencies of the carboxylate vibrations to the most likely predominant structures derived from DFT calculations has allowed a qualitative assessment of the differences in the monomeric and polymeric complexes. The analysis shows an increase of the monodentate coordination upon polymer formation. Any further quantitative decomposition of the experimental spectra into a multitude of structurally defined components would be highly speculative as the polymeric state does not provide sufficient narrow vibrational features to allow correlating experimental data to more subtle structural differences. The existence of a variety of structures in addition to the two predominant complexes appears nevertheless to be a typical property of the Eu-mediated cross-linking of BTC that leads to the large observed IR band widths. Importantly, however, we have shown here that formation of the monomer and polymer could be temporally resolved by time-dependent ITC showing that the energetics of the additional bridging Eu^{3+} coordination is largely independent of the initial coordination in the monomer and of long-range electrostatic attraction between the trivalent cation and the noncoordinating carboxylates of BTC. This indicates the prevalent role of the entropy gain by water release from the Eu^{3+} aquo ion. Contributions of water to the entropy increase upon water release from the interface of interacting biomolecules have been studied in detail and are typically accompanied by a negative ΔC_p.[48,49] Here, water release contributes to entropy increase as well but is linked to a positive ΔC_p (see Table 3). Thus, the combination of TRLFS and ITC reveals a fundamentally different solvent solute interaction in the structured hydration shell of the lanthanide as compared to the more strongly bound structured water at hydrophobic surfaces. These observations render the initial speciation of lanthanides and actinides a key determinant in their environmental immobilization by humic acids rather than structural or electrostatic constraints inherent to the humic acids.

SUMMARY

The combination of spectroscopy, calorimetry, and DFT calculations has revealed a structurally and thermodynamically consistent picture of the formation of the Eu−BTC complex under conditions that are (radio)ecologically relevant for the metal-induced polymerization of humic acids. Importantly, isothermal as well as temperature-dependent studies of the binding equilibrium are required to fully describe metal complex formation in the polymerization-promoting regime. The corresponding merits and limitations of calorimetric and spectroscopic determination of thermodynamic data have been demonstrated.

ASSOCIATED CONTENT

Supporting Information. Luminescence lifetimes of Eu−BTC spectrophotometric titration series at different temperatures (Table S1); schematic views of the complexes which have been obtained by DFT calculations including energy differences of the structures (Figure S1); IR spectra of BTC and Eu−BTC complexes obtained by DFT calculations (Figure S2). This material is available free of charge via the Internet at http://pubs.acs.org.

AUTHOR INFORMATION

Corresponding Author

*Phone: +49-351-260-3136. Fax: +49-351-260-3553. E-mail: a.barkleit@hzdr.de.

ACKNOWLEDGMENT

This work was partly supported by the German Federal Ministry of Economy (BMWi) under contract number 02E10417.

The authors acknowledge generous allocation of CPU time on supercomputers at the Zentrum für Informationsdienste und Hochleistungsrechnen (ZIH), Technische Universität Dresden, Germany.

REFERENCES

(1) Dube, A.; Zbytniewski, R.; Kowalkowski, T.; Cukrowska, E.; Buszewski, B. *Pol. J. Environ. Stud.* **2001**, *10*, 1–10.
(2) Hiraide, M. *Anal. Sci.* **1992**, *8*, 453–459.
(3) Bubb, J. M.; Lester, J. N. *Sci. Total Environ.* **1991**, *100*, 207–233.
(4) Harter, R. D.; Naidu, R. *Soil Sci. Soc. Am. J.* **2001**, *65*, 597–612.
(5) Nagendran, A.; Vijayalakshmi, A.; Arockiasamy, D. L.; Shobana, K. H.; Mohan, D. *J. Hazard. Mater.* **2008**, *155*, 477–485.
(6) Gadd, G. M. *J. Chem. Technol. Biotechnol.* **2009**, *84*, 13–28.
(7) Hummel, W.; Puigdomenech, I.; Rao, L. F.; Tochiyama, O. *C. R. Chim.* **2007**, *10*, 948–958.
(8) Tian, G. X.; Martin, L. R.; Rao, L. F. *Inorg. Chem.* **2010**, *49*, 10598–10605.
(9) Jain, A.; Yadav, K.; Mohapatra, M.; Godbole, S. V.; Tomar, B. S. *Spectrochim. Acta, A: Mol. Biomol. Spectrosc.* **2009**, *72*, 1122–1126.
(10) Matynia, A.; Lenoir, T.; Causse, B.; Spadini, L.; Jacquet, T.; Manceau, A. *Geochim. Cosmochim. Acta* **2010**, *74*, 1836–1851.
(11) Choppin, G. R. *Radiochim. Acta* **1992**, *86*, 113–120.
(12) Majumdar, A.; Biswas, M. *Polym. Bull.* **1991**, *26*, 145–150.
(13) Cao, R.; Sun, D. F.; Liang, Y. C.; Hong, M. C.; Tatsumi, K.; Shi, Q. *Inorg. Chem.* **2002**, *41*, 2087–2094.
(14) Khan, N. A.; Haque, M. M.; Jhung, S. H. *Eur. J. Inorg. Chem.* **2010**, 4975–4981.
(15) Tan, X. L.; Wang, X. K.; Geckeis, H.; Rabung, T. *Environ. Sci. Technol.* **2008**, *42*, 6532–6537.
(16) Kumke, M. U.; Eidner, S.; Krüger, T. *Environ. Sci. Technol.* **2005**, *39*, 9528–9533.
(17) Wang, Z. M.; van de Burgt, L. J.; Choppin, G. R. *Inorg. Chim. Acta* **1999**, *293*, 167–177.

(18) Rao, L. F. *Chem. Soc. Rev.* **2007**, *36*, 881–892.
(19) Rao, L. F.; Tian, G. X. *Inorg. Chem.* **2009**, *48*, 964–970.
(20) Choppin, G. R.; Rizkalla, E. N.; Elansi, T. A.; Dadgar, A. *J. Coord. Chem.* **1994**, *31*, 297–304.
(21) Gans, P.; Sabatini, A.; Vacca, A. *Talanta* **1996**, *43*, 1739–1753.
(22) *OriginPro 7.5G SR6*; OriginLab Corp.: Northhampton, MA, 2006.
(23) Moll, H.; Johnsson, A.; Schäfer, M.; Pedersen, K.; Budzikiewicz, H.; Bernhard, G. *Biometals* **2008**, *21*, 219–228.
(24) Binstead, R. A.; Zuberbühler, A. D.; Jung, B. *SPECFIT Global Analysis System*, Version 3.0.37; Spectrum Software Associates: Marlborough, MA, 2005.
(25) Kimura, T.; Choppin, G. R. *J. Alloys Compd.* **1994**, *213-214*, 313–317.
(26) Frisch, M. J.; Trucks, G. W.; Schlegel, H. B.; Scuseria, G. E.; Robb, M. A.; Cheeseman, J. R.; Montgomery, J. A., Jr.; Vreven, T.; Kudin, K. N.; Burant, J. C.; Millam, J. M.; Iyengar, S. S.; Tomasi, J.; Barone, V.; Mennucci, B.; Cossi, M.; Scalmani, G.; Rega, N.; Petersson, G. A.; Nakatsuji, H.; Hada, M.; Ehara, M.; Toyota, K.; Fukuda, R.; Hasegawa, J.; Ishida, M.; Nakajima, T.; Honda, Y.; Kitao, O.; Nakai, H.; Klene, M.; Li, X.; Knox, J. E.; Hratchian, H. P.; Cross, J. B.; Bakken, V.; Adamo, C.; Jaramillo, J.; Gomperts, R.; Stratmann, R. E.; Yazyev, O.; Austin, A. J.; Cammi, R.; Pomelli, C.; Ochterski, J. W.; Ayala, P. Y.; Morokuma, K.; Voth, G. A.; Salvador, P.; Dannenberg, J. J.; Zakrzewski, V. G.; Dapprich, S.; Daniels, A. D.; Strain, M. C.; Farkas, O.; Malick, D. K.; Rabuck, A. D.; Raghavachari, K.; Foresman, J. B.; Ortiz, J. V.; Cui, Q.; Baboul, A. G.; Clifford, S.; Cioslowski, J.; Stefanov, B. B.; Liu, G.; Liashenko, A.; Piskorz, P.; Komaromi, I.; Martin, R. L.; Fox, D. J.; Keith, T.; Al-Laham, M. A.; Peng, C. Y.; Nanayakkara, A.; Challacombe, M.; Gill, P. M. W.; Johnson, B.; Chen, W.; Wong, M. W.; Gonzalez, C.; Pople, J. A. *Gaussian 03*, Revision D.01; Gaussian, Inc.: Wallingford CT, 2004.
(27) Barone, V.; Cossi, M. *J. Phys. Chem. A* **1998**, *102*, 1995–2001.
(28) Bondi, A. *J. Phys. Chem.* **1964**, *68*, 441–451.
(29) Dolg, M.; Stoll, H.; Savin, A.; Preuss, H. *Theor. Chim. Acta* **1989**, *75*, 173–194.
(30) Krishnan, R.; Binkley, J. S.; Seeger, R.; Pople, J. A. *J. Chem. Phys.* **1980**, *72*, 650–654.
(31) Cao, Z. J.; Balasubramanian, K.; Calvert, M. G.; Nitsche, H. *Inorg. Chem.* **2009**, *48*, 9700–9714.
(32) Toraishi, T.; Nagasaki, S.; Tanaka, S. *THEOCHEM: J. Mol. Struct.* **2005**, *757*, 87–97.
(33) Denecke, M. A.; Rossberg, A.; Panak, P. J.; Weigl, M.; Schimmelpfennig, B.; Geist, A. *Inorg. Chem.* **2005**, *44*, 8418–8425.
(34) Purdie, N.; Tomson, M. B.; Riemann, N. *J. Solution Chem.* **1972**, *1*, 465–476.
(35) Fanghänel, T.; Kim, J. I. *J. Alloys Compd.* **1998**, *271*, 728–737.
(36) Kim, J. I.; Klenze, R.; Wimmer, H.; Runde, W.; Hauser, W. *J. Alloys Compd.* **1994**, *213/214*, 333–340.
(37) Heller, A.; Barkleit, A.; Bernhard, G. *Inorg. Chim. Acta* **2009**, *362*, 1215–1222.
(38) Plancque, G.; Moulin, V.; Toulhoat, P.; Moulin, C. *Anal. Chim. Acta* **2003**, *478*, 11–22.
(39) Barkleit, A.; Geipel, G.; Acker, M.; Taut, S.; Bernhard, G. *Spectrochim. Acta, A: Mol. Biomol. Spectrosc.* **2011**, *78*, 549–552.
(40) Curini, R.; D'Ascenzo, G.; De Robertis, A.; De Stefano, C.; Sammartano, S. *Thermochim. Acta* **1990**, *173*, 25–41.
(41) De Robertis, A.; De Stefano, C. *Talanta* **1991**, *38*, 439–444.
(42) Reineke, T. M.; Eddaoudi, M.; Fehr, M.; Kelley, D.; Yaghi, O. M. *J. Am. Chem. Soc.* **1999**, *121*, 1651–1657.
(43) Biswas, M.; Mukherjee, A. . In *Photoconduction Polymers/Metal-Containing Polymers*; Springer-Verlag: Berlin, 1994; Vol. 115, pp 89−123.
(44) Qin, C.; Wang, X. L.; Wang, E. B.; Su, Z. M. *Inorg. Chem.* **2005**, *44*, 7122–7129.
(45) Liu, Y. Y.; Ma, J. F.; Yang, J.; Su, Z. M. *Inorg. Chem.* **2007**, *46*, 3027–3037.
(46) Brittain, H. G. *J. Inorg. Nucl. Chem.* **1979**, *41*, 567–569.
(47) Ren, H. J.; Liu, G. X.; Cui, Z. F.; Hong, G. Y. *J. Rare Earth* **2006**, *24*, 167–170.
(48) Baldwin, R. L. *Proc. Natl. Acad. Sci. U.S.A.* **1986**, *83*, 8069–8072.
(49) Sturtevant, J. M. *Proc. Natl. Acad. Sci. U.S.A.* **1977**, *74*, 2236–2240.